Colloids and Surfaces B: Biointerfaces 262 (2026) 115538

Contents lists available at ScienceDirect

Colloids and Surfaces B: Biointerfaces

journal homepage: www.elsevier.com/locate/colsurfb

Apolipoprotein E-enriched protein corona enhances the blood–brain barrier transport of β-sheet-breaker peptide-functionalized gold nanoparticles

Simón Guerrero [a,b,*], Natalia Hassan [c,d,e], Edison Salas-Huenuleo [f], Italo Moglia [g], Roger Prades [h], Solange Massa [i], Meritxell Teixido [j], Fanny Guzman [k], Ernest Giralt [h,l,m], Fernando Albericio [m,n], Eliandre de Oliveira [o], Eyleen Araya [p,**], Marcelo J. Kogan [a,d,*]

[a] Facultad de Ciencias Químicas. y Farmacéuticas, Universidad de Chile, Santiago, Chile
[b] Facultad de Medicina, Universidad de Atacama, Copiapó, Chile
[c] Instituto Universitario de Investigación y Desarrollo Tecnológico (IDT), Universidad Tecnológica Metropolitana, Santiago, Chile
[d] Advanced Center for Chronic Diseases (ACCDis), Santiago, Chile
[e] Millenium Nucleus in NanoBioPhysics, Valparaíso, Chile
[f] Advanced Integrated Technologies (AINTECH), Santiago, Chile
[g] Facultad de Ciencias Naturales, Matemáticas y del Medio Ambiente, Universidad Tecnológica Metropolitana, Chile
[h] Institute for Research in Biomedicine (IRB Barcelona), Barcelona, Spain
[i] Department of Otolaryngology—Head & Neck Surgery, Stanford University School of Medicine, Stanford, CA, USA
[j] Gate2Brain, Barcelona Science Park, Barcelona, Spain
[k] Curauma Biotechnology Center, PontificiaUniversidad Católica de Valparaíso, Valparaíso, Chile
[l] Institute of Science and Technology (BIST), Barcelona, Spain
[m] Department of Inorganic and Organic Chemistry, University of Barcelona, Barcelona, Spain
[n] Peptide Science Laboratory, School of Chemistry andPhysics, University of KwaZulu-Natal, South Africa
[o] Proteomics Platform, Barcelona Science Park, Barcelona, Spain
[p] Departamento de Ciencias Quimicas, Facultad de Ciencias Exactas, Universidad Andres Bello, Santiago, Chile

ARTICLE INFO

Keywords:
Protein corona
Apolipoprotein E
Drug-delivery: Blood-brain barrier Transcytosis
Gold nanoparticles
#amp
#x003B2
-sheet-breaker peptides
Alzheimer'
S disease

ABSTRACT

The transient, heterogeneous nano-bio interface defined by the protein corona in biological environments dictates the biodistribution, immune recognition, metabolism, and clearance of nanomaterials. Far from being a drawback, this corona can be harnessed for targeted nanodrug delivery when its composition is predictably tuned or deliberately modulated. We hypothesized that preloading apolipoprotein E (ApoE), previously identified as a constituent of the corona of β-sheet-breaker peptide-functionalized gold nanoparticles (AuNPs), would enhance transport across the blood-brain barrier (BBB) and increase brain uptake. To test this, we synthesized AuNPs (approximately 12 nm) functionalized (AuNP-f) with CLPFFD or THRPPMWSPVWPCLPFFD peptides, both containing the β-sheet-breaker motif LPFFD, which recognizes β-amyloid aggregates implicated in Alzheimer's disease. After incubation with human plasma, hard-corona proteins were profiled by 2D IEF/SDS-PAGE and LC-MS/MS. Proteins were ranked based on their roles in nanoparticle trafficking and BBB transcytosis, and ApoE was selected for deliberate enrichment due to its recurrent presence. ApoE-decorated AuNP-f were evaluated in an *in vitro* BBB model and *in vivo* biodistribution assays using Sprague-Dawley rats. Brain accumulation was assessed *ex vivo*. Preloading ApoE onto AuNP-f significantly enhanced nanoparticle transport across the BBB *in vitro* and increased brain accumulation in rats. These results demonstrate that rational corona enrichment with ApoE improves BBB transit and brain accumulation without altering nanoparticle surface chemistry. Corona engineering thus offers a pragmatic route to brain-targeted nanodrug delivery and may be extended to other protein-receptor axes for organ-specific targeting.

* Corresponding authors at: Facultad de Ciencias Químicas. y Farmacéuticas, Universidad de Chile, Santiago, Chile.
** Corresponding author at:.Advanced Center for Chronic Diseases (ACCDis), Santiago, Chile.
E-mail addresses: simon.guerrero@ciq.uchile.cl (S. Guerrero), eyleen.araya@unab.cl (E. Araya), mkogan@ciq.uchile.cl (M.J. Kogan).

https://doi.org/10.1016/j.colsurfb.2026.115538
Received 10 September 2025; Received in revised form 15 January 2026; Accepted 7 February 2026
Available online 13 February 2026
0927-7765/© 2026 Elsevier B.V. All rights are reserved, including those for text and data mining, AI training, and similar technologies.

1. Introduction

Over the past two decades, nanotechnology in biomedical approaches has striven to unravel the biological complexity that governs the performance of novel bio-tools for pharmaceutical and medical applications. [1−4] The development of Alzheimer's disease (AD) treatments has garnered interest towards nanotechnology; one such approach involves the use of gold nanoparticles (AuNPs) functionalized with β-sheet-breaker peptides (AuNP-f) that selectively bind to β-amyloid (Aβ) aggregates and promote their disassembly, thus attenuating their neurotoxicity. These pathological aggregates are lodged behind the blood-brain barrier (BBB), a highly selective endothelial interface that blocks ≥ **98 %** of circulating therapeutics from reaching the brain. [5] Overcoming this barrier and achieving efficient central nervous system (CNS) delivery thus remains one of the foremost challenges in nanomedical AD therapy. [4,6−8]

For several years, our group has systematically optimized the brain delivery of AuNPs by tailoring their surfaces through thiol-gold chemisorption. We previously demonstrated that AuNPs functionalized with multiple copies of the β-sheet-breaker peptide CLPFFD, which binds and disrupts Aβ fibrils, quadrupled cerebral accumulation versus unmodified AuNPs (naked-AuNPs). [9,10] In a subsequent study, adding the brain-shuttle sequence THRPPMWSPVWP [11] to the N-terminus yielded the hybrid peptide THRPPMWSPVWP-CLPFFD and boosted brain uptake by ~20-fold. [7,12] Despite these gains, the absolute delivery to the CNS is only ≈ 0.3 % of the injected dose, underscoring the need for further strategies to breach the BBB more efficiently.

Upon entering the bloodstream, nanoparticles (NPs) rapidly adsorb plasma proteins, generating a dynamic protein corona that endows them with a new biological identity. [13,14] This transformation may significantly affect NPs behavior *in vivo*, modulating circulation half-life, immunogenicity, clearance by the mononuclear phagocyte system (MPS), or organ biodistribution, leading to retention in organs like the liver and spleen and altering their systemic residence time, thereby reducing their delivery to specific targets. [15−17] On the one hand, opsonization can tag NPs for rapid sequestration by the MPS, accelerating hepatic and splenic clearance while sharply reducing delivery to privileged sites, including solid tumors or harder-to-reach locations such as β-amyloids inside the CNS. Conversely, selective enrichment of "stealth" or trafficking ligands can prolong circulation and steer receptor-mediated transcytosis across biological barriers, enhancing certain treatments. [16,18−22] Thus, a detailed grasp of NPs behavior *in vivo*, particularly regarding the composition and spatiotemporal dynamics of the protein corona, is pivotal for progress in therapeutic and diagnostic nanomedicine. [23] The corona may reshape key physicochemical attributes of NPs, including hydrodynamic diameter, morphology, interfacial chemistry, surface functional groups, ζ-potential, and aggregation, thereby conferring a secondary biological identity. [24] This new identity governs NP interactions with the physiological environment, including blood, interstitial fluid, and cytoplasm, determining their cellular recognition and uptake, and ultimately dictating pharmacokinetics, organ biodistribution, and toxicological profile. [16, 25−28] Consequently, when NPs are exposed to biological media, their recognition by intended targets can be altered, potentially compromising the efficacy of rational design strategies. [29] In the case of AuNPs, their interaction with plasma proteins is governed by both kinetic and thermodynamic factors that together dictate the formation and stability of the protein corona. [30] Nevertheless, hard-corona strongly adsorbs to the NP surface via electrostatic and hydrophobic interactions and is apparently stable, remaining attached for extended periods, even in dynamic biological environments. [31] Despite dozens of studies documenting protein corona, a more limited number have deliberately engineered or pre-assembled the protein corona of NPs to bias their *in vivo* fate [32−37] Recent reviews have framed this strategy as "endogenous targeting", [38] whereby organ tropism is modulated through selective adsorption of host proteins onto nanoparticle surfaces. [39] However, applications of this concept to BBB transport and neurodegenerative disease remain comparatively scarce. This makes our strategy of preloading apolipoprotein E (ApoE) onto β-sheet-breaker peptide-functionalized AuNPs are yet a powerful approach for re-engineering corona composition and enabling efficient brain-targeted delivery. Based on these considerations, we hypothesized that peptide-functionalized AuNPs recruit endogenous ligands that shape their biological fate, and that ApoE, consistently identified in their plasma-derived corona, could act as a natural facilitator of BBB transcytosis. Therefore, we reasoned that artificially enriching the NP corona with ApoE prior to biological exposure might potentiate receptor-mediated transport across the BBB and improve brain delivery.

To evaluate this hypothesis, we first characterized the plasma-derived corona as a biologically relevant baseline to identify endogenous ligands capable of promoting translocation across the BBB into the CNS. Proteomics consistently revealed ApoE, a canonical ligand of the LDLR and LRP1 families that mediates receptor-mediated transcytosis across the BBB [8,40,41], as a prominent corona constituent. This finding motivated us to generate a deliberately engineered ApoE-enriched corona by pre-incubating AuNP-f with purified ApoE, engineering a biomimetic corona enriched in ApoE that acts as a "Trojan horse" capable of amplifying NP passage into the brain. This approach complements previous research on various strategies to traverse the BBB but is mechanistically distinct from previous strategies that involved the covalent attachment of ApoE or its mimetic peptides to nanoparticle surfaces. [42−44] Instead, our design focuses on designing new strategies based on re-engineering the biological identity of NP via controlled corona enrichment, such as "Trojan horse" tactics offering a conceptually different avenue toward brain-targeted nanomedicine, and provides a versatile blueprint for future therapeutic and diagnostic bio-tools.

2. Experimental section

Full protocols are provided in the Supplementary Information. Table S1 lists full reagent specifications and reagent catalog numbers.

2.1. Materials

Ultrapure water (Milli-Q, 18.2 MΩ cm) was used throughout. Key reagents included tetrachloroauric acid trihydrate ($HAuCl_4 \cdot x\ H_2O$, **99.995 %**, Sigma-Aldrich); sodium citrate ($Na_3C_6H_5O_7\ x \cdot 2\ H_2O$, **99.5 %**, Sigma-Aldrich); recombinant human apolipoprotein E3 (ApoE, ≥ **90 %**, Sigma-Aldrich); and all cell-culture reagents (PBS, DMEM, FBS, and penicillin/streptomycin) were molecular biology grade. Solvents and reagents for peptide synthesis (DMF, DCM, ACN, Fmoc-Rink-Amide-MBHA resin, TBTU, PyBOP, HOBt, and DIPEA) were analytical grade (Iris Biotech, Calbiochem, Merck). Reagents for protein extraction were molecular biology grade; those for 2-D electrophoresis were electrophoresis grade; and LC-MS/MS solvents were HPLC analytical grade. Detailed catalogue numbers and purities are provided in Table S1 (Supporting Information).

2.2. Equipment

UV-Vis spectra were recorded on a Perkin-Elmer Lambda 25. Hydrodynamic diameters and ζ-potential were measured with a Zetasizer Nano-ZS (Malvern). Morphology was examined by transmission electron microscopy (TEM; JEOL JEM-1010, 120 kV). X-ray photoelectron spectroscopy (PHI 5500, Physical Electronics) confirmed Au-S bonding. Peptides were purified on preparative HPLC-PDA systems (Waters) and characterized by MALDI-TOF (Applied Biosystems) and HPLC-MS (Waters). Gold was quantified by ICP-MS (197 ICP-MS 7500cx, Agilent). Protein corona composition was analyzed by two-dimensional gel electrophoresis (2-DE) using isoelectric focusing (IEF) followed by SDS-PAGE (Ettan IPGphor™, GE Healthcare) and MALDI-TOF/TOF (Applied Biosystems) or LC-MS/MS (UPLC system nanoAcquity; Waters and mass

spectrometer OrbitrapVelos; Thermo Scientific). Cell fluorescence was read on a Fluoroskan Ascent™ plate reader and whole-brain fluorescence on an in vivo FX PRO imager (Bruker). Gold content was quantified by neutron activation analysis [NAA, RECH-1 reactor, CChEN with electron flux of $2–4 \times 10^{13}$ n/(cm^2S) by 15–25 h]. Transendothelial electrical resistance (TEER) was monitored with a Millicell-ERS ohmmeter.

2.3. Methods

2.3.1. Gold nanoparticle synthesis and peptide functionalization

Citrate-stabilized AuNPs (~12 nm) were synthesized by the Turkevich-Levy method [45,46], and their size was verified by Dynamic Light Scattering (DLS) and TEM (Figure S1 and Table S4). β-Sheet-breaker peptides, CLPFFD, and the brain-shuttle chimera THRPPMWSPVWPCLPFFD were obtained by Fmoc solid-phase chemistry (> 95 % purity) [47] and characterized by HPLC-MS and MALDI-TOF (Supporting Figure S2-S3 and Table S2). Peptides were chemisorbed onto AuNPs through the N-terminal cysteine, yielding the AuNP-f conjugates. [9,10,12,46,48,49] Successful functionalization and stability were confirmed by X-ray photoelectron spectroscopy (XPS) (Figure S4 and Table S3) and DLS (Supporting Table S4), while ligand density was determined by amino acid analysis and gold quantification via ICP/MS. [10,12,48] (Table S5). For more details, refer to the protocols in Supporting Figures S1-S4.

2.3.2. Cell viability assay

Bovine brain endothelial cells (BBEC; purchased from Lonza Bioscience), rat astrocytes (obtained directly from newborn Wistar rats), or SH SY5Y neuroblastoma cells (ATCC® CRL-2266™) were seeded in 96-well plates (3×10^3 cells/well, DMEM + **10 %** FBS) and allowed to attach for 24 h (37 °C, 5 % CO_2). Cells were treated for 24 h with AuNP-f (1, 2.5, and 5 nM). Viability was assessed with the MTS/PMS assay (Promega), following the manufacturer's protocol. Absorbance was read at 490 nm (reference: 655 nm). Results represent the mean ± SD of three independent experiments (n = 3 each).

2.3.3. Formation and proteomic analysis of the protein corona

Protein analyses were conducted using non-perturbing methods for the NM-protein complex. Initially, centrifugation served as the separation strategy. However, there is uncertainty about the presence of low-affinity proteins, providing assurance only for the identification of hard-corona proteins. [50] For incubation, the AuNP-f conjugates (5 nM) were mixed 1:1 with human plasma (approved by the University of Chile Blood Bank) and incubated for 24 h at 37 °C. Nanoparticle-protein complexes were pelleted (16100 × g, 45 min) and washed twice with PBS (10 mM; pH 7.4) and once with ultrapure water. For protein extraction, pellets were resuspended in 8 M urea/2 % CHAPS (1:40 v/v), sonicated for 30 min, and shaken for 2 h at room temperature. After centrifugation, supernatants were recovered for analysis. For identification by 2-DE, isoelectric focusing (IEF) was followed by SDS-PAGE (2-DE IEF/SDS-PAGE). [51] Fifty μg of protein were separated on 7 cm IPG strips (pH 3–10 NL), followed by 10 % SDS-PAGE. Gels were silver-stained, and protein spots were excised, trypsin-digested, and identified by MALDI-TOF/TOF. Whole extracts were also digested in solution and analyzed by LC-MS/MS. Spectra were queried against the UniProt human database (Mascot; peptide tolerance 70 ppm, fragment tolerance 0.25 Da, FDR < 1 %). [52] For more protocol details, refer to Protocol S5.

2.3.4. Fluorescent labelling and ApoE preloading corona

The AuNP-f conjugates (1 mL, 5 nM) were incubated with AlexaFluor 750 NHS ester (100 μg in 200 μL DMF) for 2 h at room temperature, protected from light. Labeled particles were purified by two centrifugation/wash cycles (16100 × g, 15 min, 1.2 mM citrate). For corona enrichment, 125 μg mL^{-1} human ApoE was added to labelled AuNP-f (2.5 mL) and incubated for 1 h at 37 °C. Unbound protein was removed by centrifugation. ApoE loading was quantified by MicroBCA in supernatants. For more protocol details, refer to Protocol S7. AuNP were pre-incubated with ApoE (hereafter AuNP@ApoE), AuNP-CLPFFD were pre-incubated with ApoE (hereafter AuNP-CLPFFD@ApoE), and AuNP-THRCLPFFD were pre-incubated with ApoE (hereafter AuNP-THRCLPFFD@ApoE).

2.3.5. In vitro blood-brain barrier model and permeability

A bovine brain microvascular endothelial cell (BBMEC)/rat astrocyte co-culture was established on collagen/fibronectin-coated Transwell® inserts (0.4 μm, 0.33 cm^2), as described by Prades et al. [12] Mature monolayers (TEER > 100 Ω cm^2; Lucifer yellow rejection > 95 %; after approximately 8 days of culture and remained above this value up to day 13–14 of culture) were exposed apically to 5 nM AuNP formulations in Ringer HEPES. After 2 h (37 °C), apical and basolateral solutions were collected for fluorescence and ICP MS. The apparent permeability coefficient (Papp) was calculated considering the amount of gold present in the basal compartments as a function of time, the insert area, and the initial concentration of NPs applied to the apical compartment. The equation employed was: Papp= (dQ/dt)*(1/A)*(1/C0) (cm/s); Where (dQ/dt) is the amount of gold present in the acceptor compartment as a function of time (mmol/s), A is the area of the insert (cm2) and C0 is the initial concentration of sample applied to the donor compartment (mmol/mL). For more protocol details, refer to Protocol S8.

2.3.6. In vivo biodistribution

All animal protocols were approved by the Ethics Committee of the Experimental Animal Center, Faculty of Chemical and Pharmaceutical Sciences, University of Chile (CBE-2012–21 CYQ-UCH/s). Male Sprague Dawley rats (200–300 g) were allocated to five groups (n = 6). Formulations (Au dose 400 μg kg^{-1}, 1 mL 200 g^{-1}) were injected intraperitoneally: (i) citrate control, (ii) AuNP CLPFFD, (iii) AuNP CLPFFD@ApoE, (iv) AuNP THRCLPFFD, and (v) AuNP THRCLPFFD@ApoE. At 2 h or 24 h post injection, rats (n = 3 per time point) were anesthetized (ketamine/xylazine 2:1), perfused with PBS, and brains were excised. Fluorescence (Alexa 750) was detected using an in vivo FX PRO, and the intensity in the regions of interest (ROI) was quantified with the Bruker MI software. Brains were then snap frozen, lyophilized, digested, and Au quantified by NAA. The results are expressed as mg Au g^{-1} tissue (mean ± SD). Statistical significance was assessed by the one-way ANOVA test with Tukey-Kramer post hoc (α = 0.05). For more protocol details, refer to Protocol S9.

2.3.7. Statistical Analysis

Data are presented as mean ± SD. Group comparisons used one-way ANOVA with Tukey-Kramer post hoc correction (α = 0.05). Significance levels: $p \leq 0.05$ (*), $p < 0.01$ (**), and $p < 0.001$ (***); $p > 0.05$ was considered nonsignificant.

2.4. Results and Discussion

In this section, we present and critically discuss the experimental results obtained for AuNP-f, focusing on their colloidal stability, protein corona composition, and ability to cross the BBB. AuNPs were selected due to their well-established suitability for photothermal therapy and neurodiagnostic applications. [10,48,53–56] Their strategic design, featuring a narrow size distribution, enables precise surface functionalization with β-sheet-breaker peptides like CLPFFD, which targets Aβ aggregates, and the chimeric peptide THRPPMWSPVWP-CLPFFD (hereafter THRCLPFFD), whose THRPPMWSPVWP motif serves as a brain-shuttle sequence that facilitates BBB transcytosis, thereby enhancing their potential for targeted neurological applications. By integrating these motifs, we engineered AuNP-f capable of both recognizing neurotoxic Aβ fibrils and traversing the BBB, thereby maximizing their therapeutic reach. [7,9,10,12,48,57] The physicochemical

characterization, detailed in Supporting materials (Figures S1-S4; Tables S1-S5 and Supporting results), confirmed that AuNP-f displayed the expected core diameter (~12 nm), monodispersity, and colloidal stability required for *in vivo* applications. [10,12] Consistent with previous studies [9,12,58], the MTS assays showed no significant cytotoxicity in BBEC, rat astrocytes and SH-SY5Y cells at concentrations up to 5 nM (Figure S5). Nonetheless, we cannot rule out subtler biological effects in the absence of system-specific *in situ* analyses. Possible concerns include perturbation of protein or enzymatic activity, unintended nutrient-drug interactions, and long-term accumulation in clearance organs [59,60], underscoring the need for comprehensive bio-evaluation beyond viability assays.

2.5. Colloidal stability of AuNP-f in biological media and protein corona formation

To determine whether AuNP-f maintain colloidal stability under biologically relevant conditions, we evaluated their interaction with plasma proteins and the formation of a protein corona. Previous studies have shown that interactions between nanoparticle surfaces and plasma proteins lead to the rapid formation of an adsorbed protein corona, which defines nanoparticle pharmacokinetics and biological fate. [16, 44] Assessing whether these interactions preserve NP stability is crucial for various biological applications. Consequently, functionalized gold nanoparticles (AuNP-f) were exposed to complex media containing human plasma proteins to evaluate potential modifications of the particles. Using DLS, we confirmed that the hydrodynamic diameter increased, indicating surface changes due to protein corona formation. [26,61] In all comparisons, this parameter increased nearly threefold compared to non-incubated particles (Table 1). The stability during a 24 h period was further assessed in plasma, PBS, and DMEM medium supplemented with 10 % FBS. Fig. 1 shows a slight shift in maximum absorbance between 2 and 4 h, which remained unchanged thereafter. Thus, the particles were modified by the protein corona just within the first few hours, supporting the idea that the increase in hydrodynamic size was not due to flocculation. [61,62] Previous reports have indicated that the formation of a protein corona can increase the stability of nanomaterials (NMs). [63] To corroborate that the NPs did not flocculate after incubation in biological media, they were analyzed using TEM microscopy [61] (Fig. 2). These images indicated that NPs were maintaining their size, with distinctive rings visible around them, potentially associated with the negative staining of proteins forming the corona. [26] Therefore, a thorough characterization of different types of nanoscale blood-injected pharmacological and imaging agents under realistic conditions is required to improve overall clinical performance.

Table 1
Evaluation of protein corona formation by the effect on the hydrodynamic diameter (Dh) in each AuNP after 24 h.

Formulation	Before plasma incubation		After 24-h blood plasma incubation	
	Dh (nm) ± SD	PDI ± SD	Dh (nm) ± SD	PDI ± SD
AuNP	18.5 ± 1.0	0.21 ± 0.05	41.8 ± 14.7	0.51 ± 0.28
AuNP-CLPFFD	22.3 ± 2.5	0.25 ± 0.12	58.0 ± 10.1	0.53 ± 0.19
AuNP-THRCLPFFD	45.4 ± 4.5	0.22 ± 0.21	110 ± 20.5	0.61 ± 0.27

* In each case, the data were obtained from three independent batches of AuNP. The triplicate values of intensity for each batch are shown, with a mathematical adjustment used between batches to derive the table value, with the Polydispersity Index (PDI) for the total samples.

2.6. Characterization of the AuNPs-f protein and elucidation of proteins that may contribute to the passage across the blood-brain barrier

The protein corona observed on NPs can be defined by differences related to changes in the surface. Therefore, identifying the specific proteins forming the corona may facilitate the prediction of NP distribution within the organism. [17] AuNPs, whether functionalized or naked, are known to interact with proteins and biological molecules, resulting in the formation of stable complexes in biological media such as plasma. In this study, we specifically analyzed the protein corona formed on AuNP-f after incubation with human plasma to identify proteins potentially involved in BBB transport. This stability is consistent with the results shown in Fig. 2. The composition of the protein corona, considering protein types, abundance, and conformation on particle surfaces, acquires relevance in relation to timing and location during blood circulation, cellular uptake, intracellular localization, and overall biodistribution. These evolving entities exhibit dynamic changes, potentially leading to unpredictable behavior, functions, and effects on the pharmacokinetics and pharmacodynamics of biomodulated NMs. [16,61,64] In this context, Yu L. et al. [65] demonstrated that pre-coating NPs with proteins derived from the plasma of healthy mice on transferrin-modified NPs significantly enhanced their active targeting ability in diseased mice. This suggests that certain proteins in healthy plasma may mediate this effect, highlighting the potential to pre-modulate the protein corona for improved therapeutic outcomes. Therefore, our work builds on this concept by experimentally identifying that adsorbed proteins onto NPs could provide valuable strategies for optimizing treatment modulation.

We were able to identify the proteins that constitute the corona following the incubation of AuNP-f with human plasma. The proteins were separated and later identified in the first step, 2-DE IEF/SDS-PAGE, as shown in Fig. 3. Proteins were identified employing database references and examined by LC-MS/MS, and total proteins were analyzed by LC-MS/MS. Table 2 summarizes the most relevant proteins identified in naked-AuNP and AuNP-f distribution, while Table S6 provides a complete list of detected proteins. [50−52,66] A significant number of opsonins (including immunoglobulins, complement proteins, and fibrinogen) was found in the protein corona of all NPs. This experimental observation is consistent with our previous *in vivo* distribution studies, where naked-AuNP, AuNP-CLPFFD, and AuNP-THRCLPFFD, accumulated predominantly in clearance organs such as the liver and spleen, likely reflecting MPS uptake. [30] Additionally, the low bioaccumulation in brain tissue [9,10,12] may be associated with the presence of opsonins. These proteins are related to the bulk accumulation of NPs in organs, such as the liver and spleen, which can interfere with the adequate distribution of many novel drug delivery systems. Therefore, these systems are often dismissed due to poor effectiveness or treatment failure. [17,37] Our results support this interpretation, as opsonins were consistently detected across all nanoparticle formulations regardless of peptide functionalization. This phenomenon can be attributed to the adsorption of the aforementioned opsonins, which contain negative charges similar to AuNPs. [67] Despite the differences among functionalized particles, their size and ζ-potential do not vary sufficiently to define distinct protein corona patterns. Accordingly, our data indicate that opsonin adsorption is largely independent of the specific peptide sequence decorating the AuNP surface. Interestingly, the results in Table 2 and Fig. 3 indicate that interactions with opsonins are independent of the peptide structures coating the AuNPs. The shape and charge variations of the utilized NPs did not alter the overall interaction pattern with opsonins.

Compared to opsonins, albumin, the major plasma protein, has been recognized as a dysopsonin that antagonizes opsonins [16], reducing the phagocytosis of NPs and opposing the action of IgG and α2 human serum glycoprotein, thereby interfering with the MPS when present in the protein corona. [68] In addition, albumin can cross the BBB by adsorptive-mediated transcytosis. [69] Consistent with Table 2 and

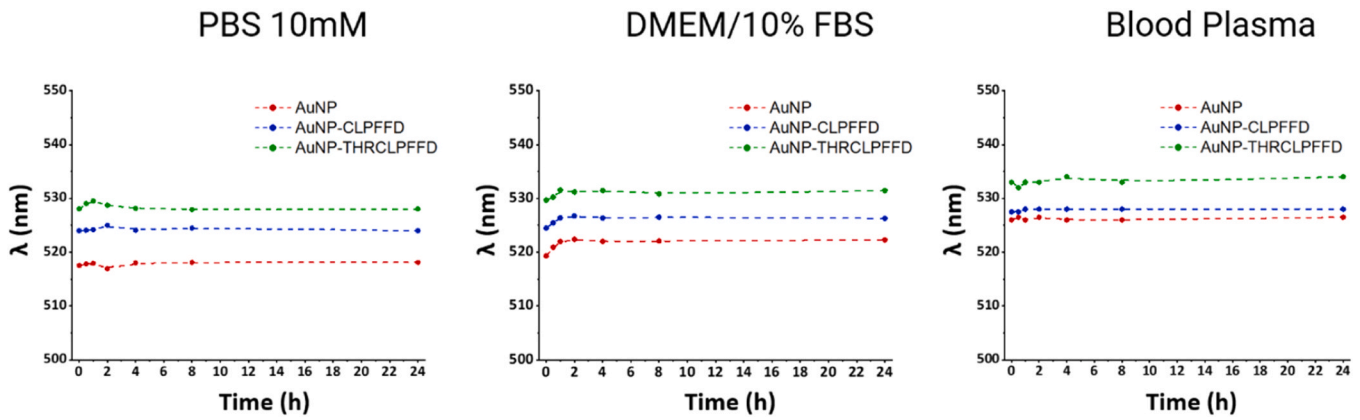


Fig. 1. Stability of AuNPs in artificial environments over a 24 h incubation period at 37 °C. Each graph indicates the value of the maximum wavelength of plasmon range absorbance. The left graph depicts incubation in 0.1 M PBS, the center graph refers to incubation with complete cell line media, and the right graph shows stability in blood plasma.

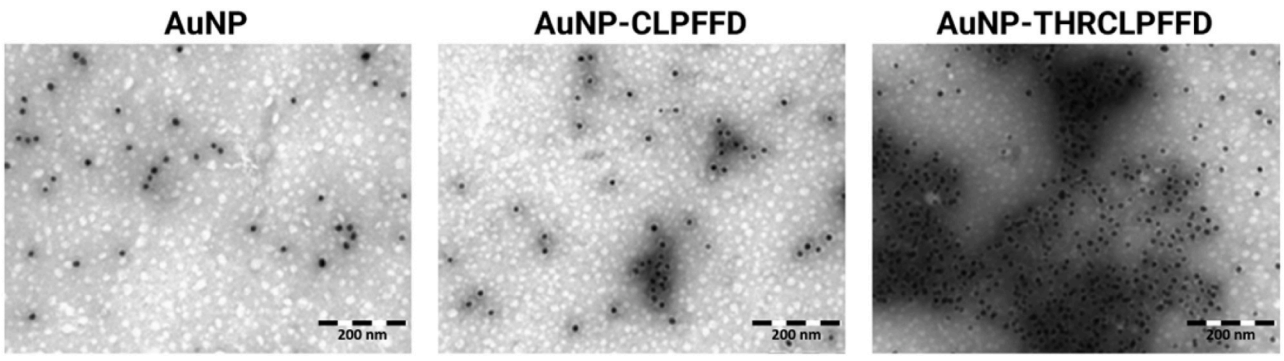


Fig. 2. TEM micrograph images obtained by transmission electron microscopy after incubation of conjugated AuNP with plasma for 24 h at 37 °C.

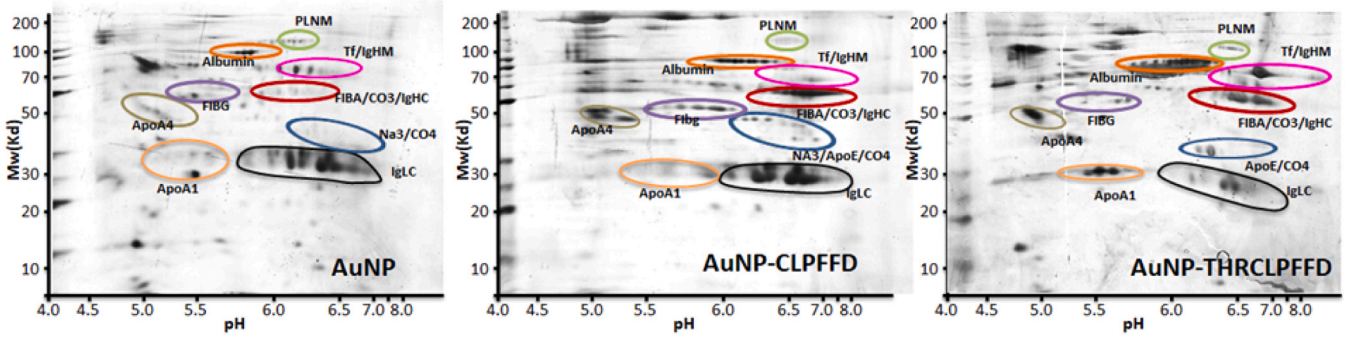


Fig. 3. Comparative analysis and identification of different proteins by 2-DE IEF/SDS-PAGE of proteins present in the CP over AuNP and AuNP-f following 24 h of incubation. Different pre-identified proteins are indicated in halos within these zones. (PLNM: Plasminogen; Tf: serotransferrin; FIBG and FIBA: β-chain and α-chain fibrinogen; IgHC and IgLC: Heavy and Light Chain Immunoglobulins; CO3 and CO4: complement proteins 3 and 4; ApoE, ApoA1, and ApoA4: apolipoproteins E, A1 and A4; NA3: possible apolipoprotein.).

Table S6, albumin was detected among the abundant components of the corona on AuNP-f. However, our data also indicate that albumin is not the only predominant protein forming the corona, and that multiple adsorbed proteins contribute to the biological identity of AuNP-f. Notably, albumin was detected at lower levels on naked-AuNP, nevertheless, even these reduced levels may still be biologically relevant and sufficient to contribute to BBB crossing, as indicated by previously reported gold levels in the brain. [9,10,12,57] Albumin was present in all particles, with major levels over AuNP-THRCLPFFD, possibly defining an essential gate of entry into the brain for these particles with the shuttle sequence THR. Likewise, other proteins interacting with naked-AuNP and AuNP-f may facilitate the delivery to various organs, especially for amphipathic species like apolipoproteins (e.g., ApoA1, ApoA4, NA3, and ApoE) found in the bloodstream. These interactions mediate the recognition of naked-AuNP and AuNP-f by specific receptors, potentially promoting transcytosis across the BBB mediated by low-density lipoprotein receptor-related protein 1 (LPR1). [8,40,41,70,71,72] Additionally, these proteins are classified as dysopsonins that help NPs evade recognition and uptake by the MPS, hence prolonging their circulation duration in the bloodstream and enhancing bioaccumulation efficiency in other organs. [16] Notably, these proteins were detected on AuNP-f but not on naked-AuNP, and their presence

Table 2
Summary of the most common proteins identified in the corona of each AuNP and AuNP-f by 2-DE IEF/SDS-PAGE and LC-MS/MS analysis. Protein content (high/moderate/low) represents a semi-quantitative qualitative classification primarily derived from the relative spot intensity/visibility in 2-DE gels. LC-MS/MS identification and Mascot scores (Table S6) support evidence to confirm protein presence and reflect confidence in identification.

	AuNP	AuNP-CLPFFD	AuNP-THRCLPFFD
Immunoglobulin	**	**	**
Fibrinogen	**	**	**
CO3	**	*	***
Albumin	**	***	***
Serotransferrin	**	***	**
Plasminogen	**	*	**
ApoE	**ND**	**	***
NA3 (possible APO)	*	*	**ND**
CO4	***	**	***
ApoA4	**	**	***
ApoA1	**	*	**
Alfa-globulins (A2MG/A1G/A2AP/ANGT)	**	**	**
Prothrombin	*	*	**
Antithrombin III	*	**	*

The asterisks indicate high (***), moderate (**) or low (*) protein content. ND: not detected.

correlates with increased gold accumulation in the brain, as previously reported. However, when bioaccumulated gold in the brain was compared in previous reports on AuNP-CLPFFD and THRCLPFFD, the shuttle sequence recognized by the transferrin receptor present in the BBB [12] could be capped by the protein corona. This masking effect could be the explanation for not getting more significant differences in NPs uptake, suggesting that endogenous proteins play a more critical role in NP biodistribution and the amphipathic nature of functionalized peptides favoring interaction with plasma proteins, leading to improved passage across the BBB in relation to naked-AuNP by promoting a more favorable protein corona that aids in transcytosis. Other proteins that can be recognized by receptors mediating receptor-mediated transcytosis include transferrin, insulin, and other proteins like albumin, which can induce a different type of transcytosis, potentially via adsorptive-mediated transcytosis, a mechanism distinct from receptor-mediated transcytosis The interaction of AuNP with plasma proteins presents many possibilities for understanding their distribution. [71,73,74] In this context, serotransferrin was detected in the protein corona of all particles. Thus, if the protein corona modulates the specific recognition of shuttle peptides towards a selected target for brain access, these proteins may account for the levels detected in previous *in vivo* assays and could explain the detection of low levels of naked-AuNP within the brain. Examining these proteins from the hard-corona and comparing them with previous reports allows the prediction of particle distribution within the organism. Modulating these interactions could enhance selectivity and drug delivery. [16,30]

2.7. Capping AuNP-f with ApoE to increase translocation across the blood-brain barrier

Previous research has defined that covalent functionalization of AuNPs with specific trafficking ligands, such as ApoE, may enhance their ability to cross the BBB and reach specific targets inside the CNS. [43,75] Although this "hard-coupling" can improve uptake in controlled settings, it imposes constraints, such as the fixed ligand layer narrowing the physicochemical design space (size, charge, and stealth coatings). Furthermore, once the NMs enter biological fluids, the covalently bound protein is rapidly cloaked by an *in situ* protein corona, which can mask receptor-binding motifs and blunt targeting efficiency. Given that the protein corona influences the distribution of NMs, preloading them with specific proteins of interest could facilitate a more targeted distribution. This has been previously demonstrated by Mahmoudi et al. [76] and Tonigold et al. [77], who reported that pre-adsorbed antibodies on NMs were not masked or displaced by the protein corona, thereby maintaining their functional interaction for controlled cellular targeting. In contrast, when covalently bound antibodies were assayed, they were covered by the protein corona, which interfered with their specific targeting functionality. [78] In our case, consistent with ApoE adsorption onto our naked-AuNP and AuNP-f formulations, the ζ-potential shifted toward less negative values and the hydrodynamic diameter increased (Table S4), supporting ApoE corona formation without clear evidence of considerable aggregation. In addition, monitoring the LSPR peak position (λ max) after ApoE incubation showed only a slight early shift, followed by stabilization up to 24 h (Figure S6). Further supporting that ApoE enrichment does not induce colloidal destabilization or aggregation.

Based on the observation that ApoE consistently appears in the plasma corona and is a canonical ligand for LRP1-mediated transcytosis, we hypothesized that enriching the corona with ApoE before biological exposure would enhance BBB transport. In this context, Human ApoE3 was selected, given its structural conservation and well-established functional role in receptor-mediated transport across the BBB. Human and rodent ApoE share approximately 75 % sequence homology and preserve key functional domains involved in lipoprotein binding and receptor interaction, [79] supporting the use of human ApoE3 in preclinical BBB transport studies and offering relevance for future translational applications. Consequently, we pre-incubated NPs with ApoE and later assessed their ability to cross the BBB using an *in vitro* model based on a co-culture of bovine brain microvessel endothelial cells and newborn rat astrocytes, which mimics the endothelial barrier of the BBB.

Following 24 h of incubation at 37 °C, ApoE was successfully separated and quantified. The binding of ApoE was ~7-fold higher on functionalized AuNPs (AuNP-f) compared to naked-AuNP. Upon disaggregation of the data, AuNP-CLPFFD exhibited an 8-fold increase in ApoE binding compared to naked-AuNP, whereas AuNP-THRCLPFFD demonstrated a 6.5-fold increase. Therefore, AuNP-CLPFFD adsorbed ≈ 1.2-fold more ApoE than its THR variant (Table S7). These differences correlate with the distinct hard-corona compositions previously observed for the same particles (Table 2 and Fig. 3).

Importantly, even before ApoE preloading, AuNP-f displays intrinsically higher permeability across the BBB model than naked-AuNP. This behavior is consistent with previous reports from our group and others showing that CLPFFD increases membrane interaction and adsorptive-mediated endocytosis. At the same time, the THRPPMWSPVWP domain further promotes receptor-associated transcytosis. These peptide-induced interfacial modifications enhance endothelial uptake and explain why AuNP-f cross the *in vitro* BBB more efficiently than unmodified citrate-stabilized AuNPs. [9,12,57] Enhanced adsorption resulted in increased translocation across the endothelial barrier, as evidenced by Fig. 4, which demonstrates that ApoE increases gold levels across the transendothelial BBB model when AuNP-f are pre-incubated with ApoE (AuNP@ApoE, AuNP-CLPFFD@ApoE, and AuNP-THRCLPFFD@ApoE), compared to non-incubated AuNP-f, which showed an approximate 1.5-fold increase. Additionally, gold levels were approximately 3.5-fold higher than those of naked-AuNP, regardless of the presence of ApoE. A detailed analysis revealed that ApoE does not alter the levels of naked-AuNP, aligning with the parameters previously documented in Table 2, suggesting that ApoE interacts only weakly with naked-AuNP and, consequently, does not induce significant changes. These findings correlate with the low levels of ApoE quantified after *in vitro* incubation with naked-AuNP, compared to AuNP-f (Table S7). In future work, it would be interesting to conduct an in-depth study of the interaction between ApoE and NP surfaces. This weak adsorption likely prevents the formation of a sufficiently enriched ApoE corona on naked AuNP, explaining why AuNP and AuNP@ApoE show no significant differences in BBB penetration in Fig. 4. These findings corroborate earlier observations that corona composition is strongly influenced by

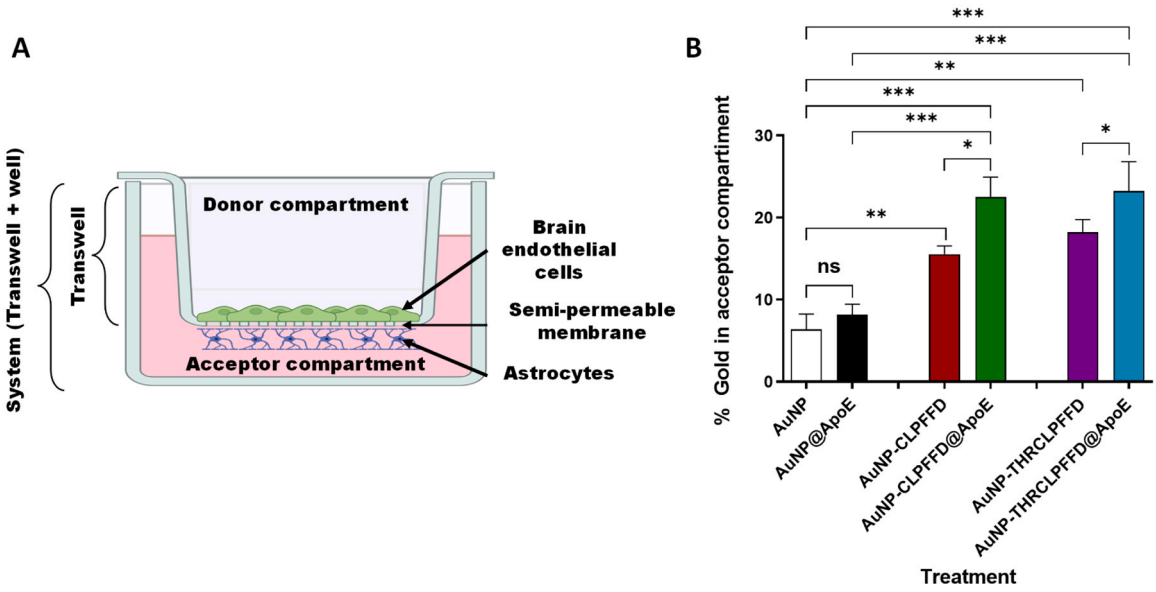


Fig. 4. Changes in AuNP levels across a trans-endothelial *in vitro* blood-brain barrier model following prior ApoE incubation to modulate the protein corona. All nanoparticle formulations were tested at the same concentration (5 nM) in the apical chamber. (A) A typical *in vitro* model of the blood-brain barrier is based on the co-culture of brain endothelial cells and astrocytes on either side of a Semi-permeable membrane (Transwell). (B) Percentage (%) of gold levels in the acceptor compartment of the *in vitro* blood-brain barrier model. Treatments without ApoE: AuNP, AuNP-CLPFFD, and AuNP-THRCLPFFD, and preincubated with ApoE: AuNP@ApoE, AuNP-CLPFFD@ApoE, and AuNP-THRCLPFFD@ApoE. Data are presented as mean ± SD (n = 3). Statistical analysis was performed using one-way ANOVA followed by Tukey's post hoc test. *, $p < 0.05$; **, $p < 0.01$; ***, $p < 0.001$; ns, not significant, and symbols indicate comparisons shown by brackets.

surface chemistry. Chuang et al. [42] previously employed the functionalization of high-density lipoprotein bearing ApoE on hydrophobic AuNPs, which were pre-coated with the polysorbate surfactant Tween 20. Under similar conditions, Jang et al. [80] observed that for hydrophilic AuNPs coated with PEG, only 5 % of the proteins forming the protein corona were HDLs, including ApoE. Our data extends this trend by showing that peptide decoration markedly enhances ApoE adsorption. These results align with the findings of Xia et al. [81], who demonstrated that ApoE co-aggregates with Aβ peptides, as CLPFFD is a β-sheet-breaker derived from an Aβ nucleation sequence [82], and its presence likely underlies the higher ApoE affinity of AuNP-f.

At this stage, it is important to consider whether preloaded ApoE in hard-corona could interfere with the targeting function of the CLPFFD peptide toward β-amyloid aggregates. The CLPFFD sequence is known to recognize Aβ fibrils through sequence-specific interactions that depend on the accessibility of its active residues. Moreover, ApoE itself has been widely reported to interact with Aβ species and to modulate their aggregation and clearance pathways. [83,84] These observations suggest that the presence of an ApoE-enriched corona is not necessarily interfering with CLPFFD-mediated recognition of Aβ, and at the same time, ApoE enrichment primarily facilitates receptor-mediated BBB transcytosis, while the CLPFFD motif is expected to remain available to interact with Aβ once the nanoparticles reach the brain parenchyma. This dual functionality supports the rationale of ApoE preloading as a

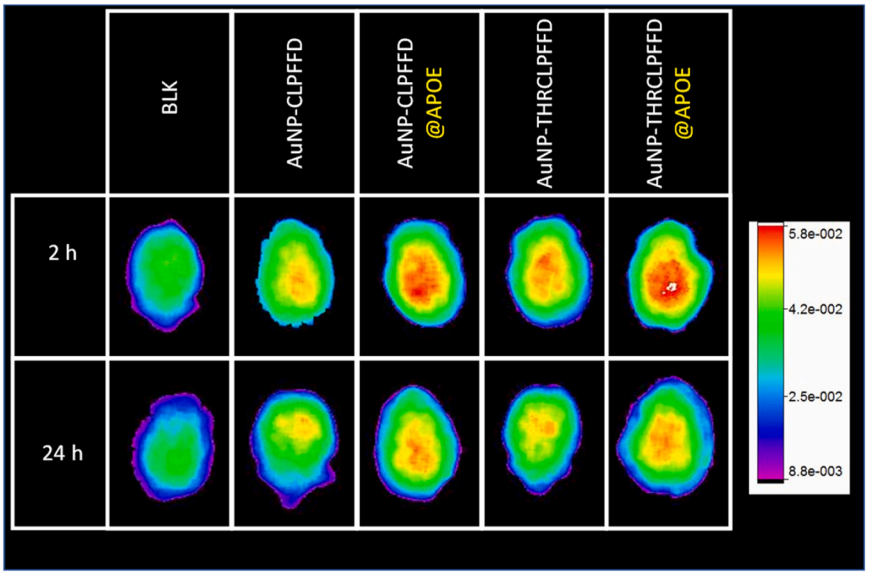


Fig. 5. Fluorescence of *ex-vivo* rat brains. A comparison of rat brains subjected to different AuNP treatments at 2 h and 24 h after intraperitoneal administration; levels are expressed as fluorescence counts. Treatments were labeled with Alexa fluor 750. Treatments: Vehicle control (BLK); AuNP-CLPFFD and pre-incubated with ApoE (AuNP-CLPFFD@ApoE); AuNP-THRCLPFFD and pre-incubated with ApoE (AuNP-THRCLPFFD@ApoE).

complementary, rather than conflicting, strategy.

Considering that ApoE on AuNP-f can alter the levels crossing the BBB, it is essential to confirm whether modulating the protein corona could influence distribution and introduce new strategies for drug delivery. In previous reports, we demonstrated that AuNPs reach the brain, and that functionalization with peptides increases their levels in the brain, possibly through peptide-mediated interactions with BBB components (e.g., membrane affinity and receptor-associated transport). However, since protein corona formation occurs spontaneously upon biological exposure, the corona may further modulate nanoparticle biological identity and indirectly influence biodistribution and brain accumulation. [7,10,12,57] Therefore, interaction with proteins able to cross the BBB is hypothesized to increase brain gold levels. As shown in Fig. 5 and Fig. 6, brains collected 2 and 24 h after intraperitoneal injection of AuNP-f exhibited differences in fluorescence levels when the NPs were pre-incubated with ApoE. Increased fluorescence levels were detected using Alexa 750 on NPs. Fluorescence intensity was higher 2 h after treatment, consistent with previous reports. [9,10,12,57] These results align with observed differences and the gradual decrease in fluorescence levels over time. Gold levels in the brain were evaluated using neutronic activation to confirm the presence of AuNP-f, as shown in Fig. 7. These results demonstrate that ApoE enhances AuNP-f levels by approximately 2-fold in the protein corona. Notably, around 1 % of the administered dose reached the brain after intraperitoneal administration, as quantified by neutron activation analysis. Also has been quantified Au and expressed as %ID in other organs (Table S8), all these data are correlated with *ex vivo* fluorescence imaging (Figure S7). The levels of gold of AuNP-f are approximately one order of magnitude higher than that of naked-AuNPs reported in our previous studies under comparable conditions [12], and further supports that peptide functionalization and corona modulation can significantly improve CNS delivery even under a restrictive administration route. This distribution paralleled that of NMs injected into the bloodstream to target tumors, with meta-analyses indicating that roughly 0.7 % of the administered dose reached the target. [85,86] Thus, our proposed methods demonstrate comparable

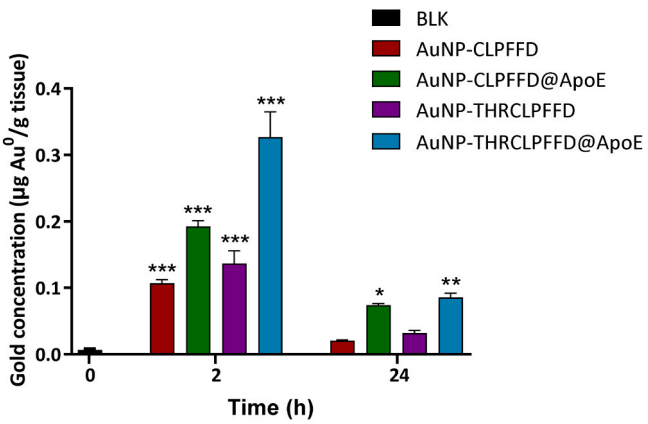


Fig. 7. Determination of gold content by *ex vivo* neutron activation, comparing gold levels in the brains of rats subjected to different treatments, at 2 h and 24 h after administration. Vehicle control (BLK). N = 3, the sample standard deviation is plotted. Statistical analysis was performed using one-way ANOVA followed by Tukey's post hoc test. * $p < 0.05$; ** $p < 0.01$; and *** $p < 0.001$. Significance symbols indicate comparisons to the corresponding control without treatment.

efficiency, even with intraperitoneal administration. Interestingly, Dal Magro et al. [84], employed a similar strategy using a pre-formed "artificial protein corona". The lipidic NPs coated with polysorbate 80 and later incubated for 15 min with ApoE4, reached nearly 1 % delivery to the brain, which is 3-fold more than that of undecorated particles previously incubated with ApoE4. In our study, we selected ApoE3, considering that ApoE4 is associated with Alzheimer's disease. Additionally, our administration route was intraperitoneal, a more challenging pathway due to the first-pass effect. These findings confirm the feasibility of modulating a robust protein and achieving similar results with different types of NPs.

In another context, Zhang et al. [83] used polymeric nanomicelles as

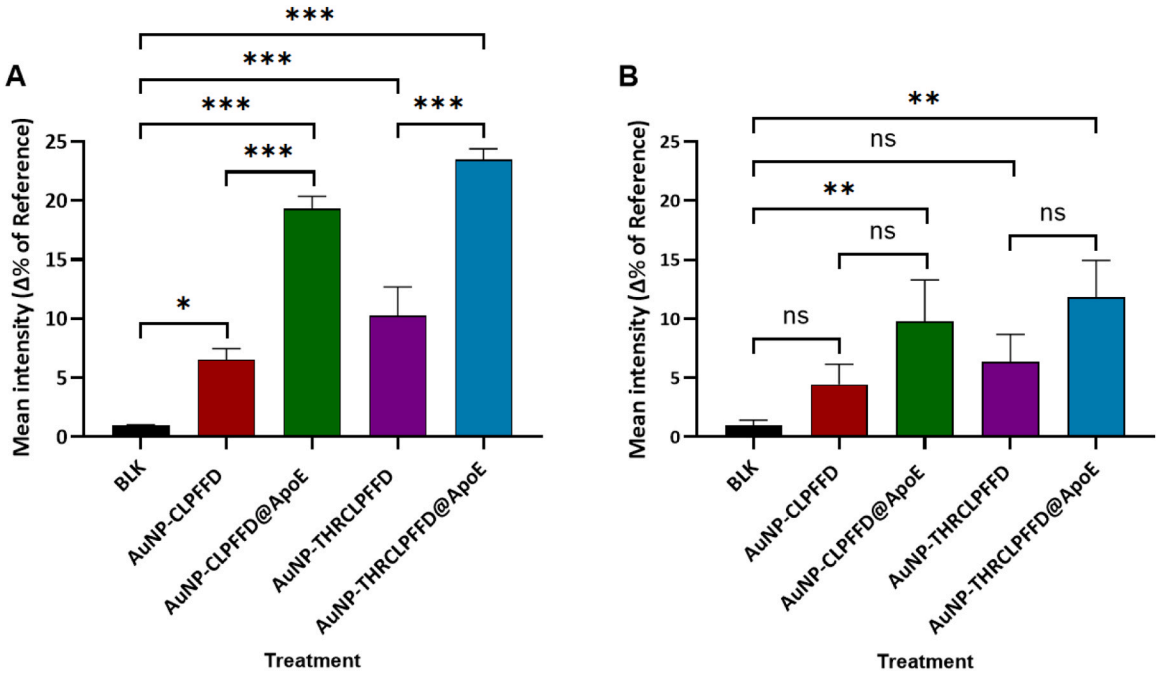


Fig. 6. Determination of *ex-vivo* fluorescence, comparing fluorescence levels in rat brains treated with AuNP-CLPFFD, AuNP-CLPFFD pre-incubated with ApoE (AuNP-CLPFFD@ApoE), AuNP-THRCLPFFD, and AuNP-THRCLPFFD pre-incubated with ApoE (AuNP-THRCLPFFD@ApoE), labeled with Alexa fluor 750. Fluorescence values were normalized relative to the brain of a vehicle control rat (BLK; untreated and not injected with Alexa Fluor 750), at 2 h (A) and 24 h (B) after administration. N = 3, the sample standard deviation is plotted. Statistical analysis was performed using one-way ANOVA followed by Tukey's post hoc test. *, $p < 0.05$; **, $p < 0.01$; ***, $p < 0.001$; ns, not significant, and symbols indicate comparisons shown by brackets.

a drug-delivery system for paclitaxel. They successfully doubled paclitaxel levels within glioma brain cells by pre-incubating them with blood plasma and recombinant human ApoE (rhApoE) to form a hard-corona before *in vivo* administration.

A recent study by Wei et al. [87] suggests that ApoE adsorbed onto NPs may attenuate neurological oxidative stress and the inflammation observed in the ApoE -/- knockout mice model. These findings highlight the potential of utilizing ApoE-functionalized NPs for targeted drug delivery across the BBB, and its neuroprotective applications. Given the role of ApoE in modulating lipid metabolism and neuroinflammation, future studies should explore its broader implications in NP-based therapies for neurodegenerative diseases, potentially offering novel strategies to mitigate pathological processes in conditions like Alzheimer's disease and other neurological disorders.

2.8. Conclusion

Preloading ApoE to modulate the protein corona of AuNP-f significantly enhanced its delivery to the brain. This finding demonstrates that tuning the protein corona can influence NP distribution. Our results suggest that nonspecific interactions with ApoE facilitate brain penetration, and that other proteins, such as albumin or transferrin, may also contribute in alternate transport pathways. This approach represents a promising strategy for improving NP-based drug delivery to the brain. Additionally, exploring methods to minimize undesired interactions may assist in mitigating potential adverse effects. It should be noted that intraperitoneal administration represents a restrictive delivery route for brain targeting, due to extensive first-pass interactions and systemic protein exposure. Therefore, the observed enhancement in brain accumulation following ApoE corona enrichment underscores the robustness of this strategy even under demanding biodistribution conditions.

Although the protein corona is known to be dynamic and subject to remodeling during circulation, our results suggest that an ApoE-enriched hard-corona fraction remains stable at early time points to exert a measurable biological effect, as evidenced by enhanced BBB transport *in vitro* and increased brain accumulation *in vivo*. These findings support the idea that the initial hard-corona composition plays a significant role in determining early biological recognition and organ targeting, even in the presence of subsequent protein exchange. Even though the dynamic remodeling of the protein corona under physiological shear stress was not addressed in this study, future *in vivo* and microphysiological investigations, including microfluidic and organ-on-a-chip models, will be necessary to explore additional protein exchange processes that may occur during circulation and further modulate NP biodistribution in the brain and other organs.

Future research should focus on predicting the *in vivo* behaviour of NMs, particularly AuNP-f, by analysing surface modifications and their interactions with plasma proteins to enhance our understanding of their pharmacokinetics. Developing strategies to regulate these interactions according to therapeutic targets is essential, enhancing favorable interactions while minimizing undesirable ones to optimize NP delivery. Complementary biophysical studies using membrane models and protein corona analysis will provide deeper insights of the *in vivo* behaviur of AuNP-f. Ultimately, these findings will contribute to the development of machine learning and artificial intelligence models to improve the prediction of NM-based drug delivery.

Although the present study relies on established *in vitro* and *in vivo* models, species-specific differences may influence quantitative outcomes, and extrapolation to human physiology should be interpreted with caution. Future studies using fully humanized BBB models will be required to strengthen translational relevance.

CRediT authorship contribution statement

Meritxell Teixido: Writing – review & editing, Validation, Methodology, Investigation, Formal analysis, Data curation. **Solange Massa:** Writing – review & editing, Validation, Investigation, Formal analysis, Data curation. **Ernest Giralt:** Writing – review & editing, Resources, Conceptualization. **Fanny Guzman:** Writing – review & editing, Validation, Methodology, Data curation. **Roger Prades:** Writing – review & editing, Validation, Methodology, Investigation, Formal analysis, Data curation. **Italo Moglia:** Writing – review & editing, Validation, Investigation, Formal analysis, Data curation. **Edison Salas-Huenuleo:** Writing – review & editing, Validation, Investigation, Formal analysis, Data curation. **Eliandre de Oliveira:** Writing – review & editing, Validation, Methodology, Investigation, Data curation. **Fernando Albericio:** Writing – review & editing, Supervision, Resources. **Marcelo J. Kogan:** Writing – review & editing, Visualization, Validation, Resources, Methodology, Funding acquisition, Data curation, Conceptualization. **Natalia Hassan:** Writing – review & editing, Validation, Methodology, Investigation, Funding acquisition, Formal analysis, Data curation. **Eyleen Araya:** Writing – review & editing, Visualization, Supervision, Resources, Methodology, Funding acquisition, Data curation, Conceptualization. **Simón Guerrero:** Writing – review & editing, Writing – original draft, Visualization, Validation, Supervision, Resources, Project administration, Methodology, Investigation, Funding acquisition, Formal analysis, Data curation, Conceptualization.

Funding

This work was funded by FONDECYT Inicio 11221282 (SG), FONDECYT 1230303 (EA), FONDECYT 1230830 (NH), FONDECYT 1251140 (MK) and FONDAP 15130011, FONDAP Continuación 1523A0008 (MK).

Declaration of Competing Interest

The authors declare that they have no known competing financial interests or personal relationships that could have appeared to influence the work reported in this paper.

Acknowledgements

The authors would like to acknowledge The National Research and Development Agency of Chile (ANID), dependent on the Ministry of Science, Technology, Knowledge, and Innovation.

Appendix A. Supporting information

Supplementary data associated with this article can be found in the online version at doi:10.1016/j.colsurfb.2026.115538.

Data Availability

Data will be made available on request.

References

[1] AP Ramos, MAE Cruz, CB Tovani, P. Ciancaglini, Biomedical applications of nanotechnology, Biophys. Rev. 9 (2) (2017) 79–89.
[2] L.-H. Fu, J. Yang, J.-F. Zhu, M.-G. Ma, Synthesis of Gold Nanoparticles and Their Applications in Drug Delivery. In: Rai PDM, Shegokar PDR, editors. Metal Nanoparticles in Pharma, Springer International Publishing, Cham, 2017, pp. 155–191.
[3] DF Silva, ALP Melo, AFC Uchoa, GMA Pereira, AEF Alves, MC Vasconcellos, et al., Biomedical approach of nanotechnology and biological risks: a mini-review, Int J. Mol. Sci. 24 (23) (2023).
[4] R. Wang, X. Zhang, K. Feng, W. Zeng, J. Wu, D. Sun, et al., Nanotechnologies meeting natural sources: Engineered lipoproteins for precise brain disease theranostics, Asian J. Pharm. Sci. 18 (5) (2023) 100857.
[5] MA Husain, B. Laurent, M. Plourde, APOE and Alzheimer's Disease: From Lipid Transport to Physiopathology and Therapeutics, Front Neurosci. 15 (2021) 630502.
[6] CM Bellettato, M. Scarpa, Possible strategies to cross the blood–brain barrier, Ital. J. Pediatr. 44 (2) (2018) 131.

[7] P. Arranz-Gibert, R. Prades, B. Guixer, S. Guerrero, E. Araya, S. Ciudad, et al., HAI peptide and backbone analogs—validation and enhancement of biostability and bioactivity of BBB Shuttles, Sci. Rep. 8 (1) (2018) 17932.
[8] GR Topal, M. Meszaros, G. Porkolab, A. Szecsko, TF Polgar, L. Siklos, et al., ApoE-targeting increases the transfer of solid lipid nanoparticles with donepezil cargo across a culture model of the blood-brain barrier, Pharmaceutics 13 (1) (2020).
[9] S. Guerrero, E. Araya, JL Fiedler, JI Arias, C. Adura, F. Albericio, et al., Improving the brain delivery of gold nanoparticles by conjugation with an amphipathic peptide, Nanomed. (Lond.) 5 (6) (2010) 897–913.
[10] S. Guerrero, JR Herance, S. Rojas, JF Mena, JD Gispert, GA Acosta, et al., Synthesis and in vivo evaluation of the biodistribution of a 18F-labeled conjugate gold-nanoparticle-peptide with potential biomedical application, Bioconjug Chem. 23 (3) (2012) 399–408.
[11] JH Lee, JA Engler, JF Collawn, BA. Moore, Receptor mediated uptake of peptides that bind the human transferrin receptor, Eur. J. Biochem 268 (7) (2001) 2004–2012.
[12] R. Prades, S. Guerrero, E. Araya, C. Molina, E. Salas, E. Zurita, et al., Delivery of gold nanoparticles to the brain by conjugation with a peptide that recognizes the transferrin receptor, Biomaterials 33 (29) (2012) 7194–7205.
[13] Q. Peng, XQ Wei, Q. Yang, S. Zhang, T. Zhang, XR Shao, et al., Enhanced biostability of nanoparticle-based drug delivery systems by albumin corona, Nanomed. (Lond.) 10 (2) (2015) 205–214.
[14] A. Salvati, AS Pitek, MP Monopoli, K. Prapainop, FB Bombelli, DR Hristov, et al., Transferrin-functionalized nanoparticles lose their targeting capabilities when a biomolecule corona adsorbs on the surface, Nat. Nanotechnol. 8 (2) (2013) 137–143.
[15] MP Monopoli, C. Aberg, A. Salvati, KA. Dawson, Biomolecular coronas provide the biological identity of nanosized materials, Nat. Nanotechnol. 7 (12) (2012) 779–786.
[16] YF Wang, Y. Zhou, J. Sun, X. Wang, Y. Jia, K. Ge, et al., The Yin and Yang of the protein corona on the delivery journey of nanoparticles, Nano Res 16 (1) (2023) 715–734.
[17] Y. Ma, J. Hong, Y. Ding, Biological Behavior Regulation of Gold Nanoparticles via the Protein Corona, Adv. Health Mater. 9 (6) (2020) e1901448.
[18] AL Bailly, F. Correard, A. Popov, G. Tselikov, F. Chaspoul, R. Appay, et al., In vivo evaluation of safety, biodistribution and pharmacokinetics of laser-synthesized gold nanoparticles, Sci. Rep. 9 (1) (2019) 12890.
[19] DV Haute, JM. Berlin, Challenges in realizing selectivity for nanoparticle biodistribution and clearance: lessons from gold nanoparticles, Ther. Deliv. 8 (9) (2017) 763–774.
[20] MA. Abdelhalim, Uptake of gold nanoparticles in several rat organs after intraperitoneal administration in vivo: a fluorescence study, Biomed. Res Int 2013 (2013) 353695.
[21] PM Kelly, C. Aberg, E. Polo, A. O'Connell, J. Cookman, J. Fallon, et al., Mapping protein binding sites on the biomolecular corona of nanoparticles, Nat. Nanotechnol. 10 (5) (2015) 472–479.
[22] Q. Peng, H. Mu, The potential of protein-nanomaterial interaction for advanced drug delivery, J. Control Release 225 (2016) 121–132.
[23] Q. Peng, S. Zhang, Q. Yang, T. Zhang, XQ Wei, L. Jiang, et al., Preformed albumin corona, a protective coating for nanoparticles based drug delivery system, Biomaterials 34 (33) (2013) 8521–8530.
[24] J. Liu, Q. Peng, Protein-gold nanoparticle interactions and their possible impact on biomedical applications, Acta Biomater. 55 (2017) 13–27.
[25] G. Wang, W. Wang, E. Shangguan, S. Gao, Y. Liu, Effects of gold nanoparticle morphologies on interactions with proteins, Mater. Sci. Eng. C. Mater. Biol. Appl. 111 (2020) 110830.
[26] R. Garcia-Alvarez, M. Hadjidemetriou, A. Sanchez-Iglesias, LM Liz-Marzan, K. Kostarelos, In vivo formation of protein corona on gold nanoparticles. The effect of their size and shape, Nanoscale 10 (3) (2018) 1256–1264.
[27] T. Cedervall, I. Lynch, S. Lindman, T. Berggard, E. Thulin, H. Nilsson, et al., Understanding the nanoparticle-protein corona using methods to quantify exchange rates and affinities of proteins for nanoparticles, Proc. Natl. Acad. Sci. USA 104 (7) (2007) 2050–2055.
[28] I. Lynch, KA. Dawson, Protein-nanoparticle interactions, Nano Today 3 (1) (2008) 40–47.
[29] R. Nicoară, M. Ilieș, A. Uifălean, CA Iuga, F. Loghin, Quantification of the PEGylated Gold Nanoparticles Protein Corona. Influence on Nanoparticle Size and Surface Chemistry, Appl. Sci. [Internet] 9 (22) (2019).
[30] W. Zhang, Protein corona of nanoparticles and its application in drug delivery, in: H. Xu, Gu N (Eds.), Nanotechnology in Regenerative Medicine and Drug Delivery Therapy, Springer Singapore, Singapore, 2020, pp. 389–419.
[31] NM Mayordomo, A. Zatarain-Beraza, F. Valerio, V. Alvarez-Mendez, P. Turegano, L. Herranz-Garcia, et al., The Protein Corona Paradox: Challenges in Achieving True Biomimetics in Nanomedicines, Biomim. (Basel) 10 (5) (2025).
[32] K. Liu, R. Nilsson, E. Lazaro-Ibanez, H. Duan, T. Miliotis, M. Strimfors, et al., Multiomics analysis of naturally efficacious lipid nanoparticle coronas reveals high-density lipoprotein is necessary for their function, Nat. Commun. 14 (1) (2023) 4007.
[33] Y. Miao, L. Li, Y. Wang, J. Wang, Y. Zhou, L. Guo, et al., Regulating protein corona on nanovesicles by glycosylated polyhydroxy polymer modification for efficient drug delivery, Nat. Commun. 15 (1) (2024) 1159.
[34] C. Marques, G. Borchard, O. Jordan, Unveiling the challenges of engineered protein corona from the proteins' perspective, Int J. Pharm. 654 (2024) 123987.
[35] T. Zhao, M. Ren, J. Shi, H. Wang, J. Bai, W. Du, et al., Engineering the protein corona: Strategies, effects, and future directions in nanoparticle therapeutics, Biomed. Pharm. 175 (2024) 116627.
[36] F. Muraca, L. Boselli, V. Castagnola, KA. Dawson, Ultrasmall gold nanoparticle cellular uptake: influence of transient bionano interactions, ACS Appl. Bio Mater. 3 (6) (2020) 3800–3808.
[37] H. Li, Y. Wang, Q. Tang, D. Yin, C. Tang, E. He, et al., The protein corona and its effects on nanoparticle-based drug delivery systems, Acta Biomater. 129 (2021) 57–72.
[38] SA Dilliard, DJ. Siegwart, Passive, active and endogenous organ-targeted lipid and polymer nanoparticles for delivery of genetic drugs, Nat. Rev. Mater. 8 (4) (2023) 282–300.
[39] SA Dilliard, Q. Cheng, DJ. Siegwart, On the mechanism of tissue-specific mRNA delivery by selective organ targeting nanoparticles, Proc. Natl. Acad. Sci. USA 118 (52) (2021).
[40] N. Hartl, F. Adams, OM. Merkel, From adsorption to covalent bonding: Apolipoprotein E functionalization of polymeric nanoparticles for drug delivery across the blood-brain barrier, Adv. Ther. (Weinh.) 4 (1) (2021).
[41] DA Elliott, CS Weickert, Garner, Apolipoproteins in the brain: implications for neurological and psychiatric disorders, Clin. Lipido B (4) (2010) 555–573, 51.
[42] ST Chuang, YS Shon, V. Narayanaswami, Apolipoprotein E3-mediated cellular uptake of reconstituted high-density lipoprotein bearing core 3, 10, or 17 nm hydrophobic gold nanoparticles, Int J. Nanomed. 12 (2017) 8495–8510.
[43] ELL Yeo, JUJ Cheah, PSP Thong, KC Soo, JCY. Kah, Gold Nanorods Coated with Apolipoprotein E Protein Corona for Drug Delivery, ACS Appl. Nano Mater. 2 (10) (2019) 6220–6229.
[44] AA Ashkarran, S. Tadjiki, Z. Lin, K. Hilsen, N. Ghazali, S. Krikor, et al., Protein Corona Composition of Gold Nanocatalysts, ACS Pharmacol. Transl. Sci. 7 (4) (2024) 1169–1177.
[45] J. Turkevich, PC Stevenson, J. Hillier, A study of the nucleation and growth processes in the synthesis of colloidal gold, Discuss. Faraday Soc. 11 (0) (1951) 55–75.
[46] R. Levy, NT Thanh, RC Doty, I. Hussain, RJ Nichols, DJ Schiffrin, et al., Rational and combinatorial design of peptide capping ligands for gold nanoparticles, J. Am. Chem. Soc. 126 (32) (2004) 10076–10084.
[47] BL Nilsson, MB Soellner, RT. Raines, Chemical synthesis of proteins, Annu Rev. Biophys. Biomol. Struct. 34 (2005) 91–118.
[48] AR Guerrero, N. Hassan, CA Escobar, F. Albericio, MJ Kogan, E. Araya, Gold nanoparticles for photothermally controlled drug release, Nanomed. (Lond.) 9 (13) (2014) 2023–2039.
[49] A. Ulman, Formation and Structure of Self-Assembled Monolayers, Chem. Rev. 96 (4) (1996) 1533–1554.
[50] I. Srivastava, MS Khan, K. Dighe, M. Alafeef, Z. Wang, T. Banerjee, et al., On-Chip Electrical Monitoring of Real-Time “Soft” and “Hard” Protein Corona Formation on Carbon Nanoparticles, Small Methods 4 (7) (2020) 2000099.
[51] M. Lundqvist, J. Stigler, G. Elia, I. Lynch, T. Cedervall, KA. Dawson, Nanoparticle size and surface properties determine the protein corona with possible implications for biological impacts, Proc. Natl. Acad. Sci. USA 105 (38) (2008) 14265–14270.
[52] M. Magro, M. Zaccarin, G. Miotto, L. Da Dalt, D. Baratella, P. Fariselli, et al., Analysis of hard protein corona composition on selective iron oxide nanoparticles by MALDI-TOF mass spectrometry: identification and amplification of a hidden mastitis biomarker in milk proteome, Anal. Bioanal. Chem. 410 (12) (2018) 2949–2959.
[53] E. Araya, I. Olmedo, NG Bastus, S. Guerrero, VF Puntes, E. Giralt, et al., Gold Nanoparticles and Microwave Irradiation Inhibit Beta-Amyloid Amyloidogenesis, Nanoscale Res. Lett. 3 (11) (2008) 435.
[54] J. Ruff, N. Hassan, F. Morales-Zavala, J. Steitz, E. Araya, MJ Kogan, et al., CLPFFD-PEG functionalized NIR-absorbing hollow gold nanospheres and gold nanorods inhibit beta-amyloid aggregation, J. Mater. Chem. B 6 (16) (2018) 2432–2443.
[55] F. Morales-Zavala, P. Jara-Guajardo, D. Chamorro, AL Riveros, A. Chandia-Cristi, N. Salgado, et al., In vivo micro computed tomography detection and decrease in amyloid load by using multifunctionalized gold nanorods: a neurotheranostic platform for Alzheimer's disease, Biomater. Sci. 9 (11) (2021) 4178–4190.
[56] MP Oyarzun, A. Tapia-Arellano, P. Cabrera, P. Jara-Guajardo, MJ. Kogan, Plasmonic Nanoparticles as Optical Sensing Probes for the Detection of Alzheimer's Disease, Sens. (Basel) 21 (6) (2021).
[57] C. Velasco-Aguirre, F. Morales, E. Gallardo-Toledo, S. Guerrero, E. Giralt, E. Araya, et al., Peptides and proteins used to enhance gold nanoparticle delivery to the brain: preclinical approaches, Int J. Nanomed. 10 (2015) 4919–4936.
[58] N. Hassan, F. Oyarzun-Ampuero, P. Lara, S. Guerrero, V. Cabuil, A. Abou-Hassan, et al., Flow Chemistry to Control the Synthesis of Nano and Microparticles for Biomedical Applications, Curr. Top. Med. Chem. 14 (5) (2014) 676–689.
[59] YP Liu, S. Zhu, ZJ Gu, CY Chen, YL. Zhao, Toxicity of manufactured nanomaterials, Particuology 69 (2022) 31–48.
[60] Y. Ji, Y. Wang, X. Wang, C. Lv, Q. Zhou, G. Jiang, et al., Beyond the promise: Exploring the complex interactions of nanoparticles within biological systems, J. Hazard Mater. 468 (2024) 133800.
[61] T. Kopac, Protein corona, understanding the nanoparticle-protein interactions and future perspectives: A critical review, Int J. Biol. Macromol. 169 (2021) 290–301.
[62] R. Capomaccio, IO Jimenez, P. Colpo, D. Gilliland, G. Ceccone, F. Rossi, et al., Determination of the structure and morphology of gold nanoparticle-HSA protein complexes, Nanoscale 7 (42) (2015) 17653–17657.
[63] A. Tukova, Y. Nie, M. Tavakkoli Yaraki, NT Tran, J. Wang, A. Rodger, et al., Shape dependent protein-induced stabilization of gold nanoparticles: From a protein corona perspective, Aggregate 4 (4) (2023) e323.
[64] G. Caracciolo, OC Farokhzad, M. Mahmoudi, Biological Identity of Nanoparticles In Vivo: Clinical Implications of the Protein Corona, Trends Biotechnol. 35 (3) (2017) 257–264.

[65] L. Yu, M. Xu, W. Xu, W. Xiao, X.-h Jiang, L. Wang, et al., Enhanced Cancer-targeted Drug Delivery Using Precoated Nanoparticles, Nano Lett. 20 (12) (2020) 8903–8911.
[66] F. Pederzoli, G. Tosi, MA Vandelli, D. Belletti, F. Forni, B. Ruozi, Protein corona and nanoparticles: how can we investigate on? WIREs Nanomed. Nanobiotechnology 9 (6) (2017) e1467.
[67] V. Francia, D. Montizaan, A. Salvati, Interactions at the cell membrane and pathways of internalization of nano-sized materials for nanomedicine, Beilstein J. Nanotechnol. 11 (2020) 338–353.
[68] E. Papini, R. Tavano, F. Mancin, Opsonins and Dysopsonins of Nanoparticles: Facts, Concepts, and Methodological Guidelines, Front Immunol. 11 (2020) 567365.
[69] X. Zhu, K. Jin, Y. Huang, Z. Pang, 7 - Brain drug delivery by adsorption-mediated transcytosis. In: Gao H, Gao X, editors. Brain Targeted Drug Delivery System: Academic Press, 2019, pp. 159–183.
[70] A. Wunsch, D. Mulac, K. Langer, Lipoprotein imitating nanoparticles: Lecithin coating binds ApoE and mediates non-lysosomal uptake leading to transcytosis over the blood-brain barrier, Int J. Pharm. 589 (2020) 119821.
[71] X. Gao, J. Xu, T. Yao, X. Liu, H. Zhang, C. Zhan, Peptide-decorated nanocarriers penetrating the blood-brain barrier for imaging and therapy of brain diseases, Adv. Drug Deliv. Rev. 187 (2022) 114362.
[72] S. Masoudi Asil, J. Ahlawat, G. Guillama Barroso, M. Narayan, Nanomaterial based drug delivery systems for the treatment of neurodegenerative diseases, Biomater. Sci. 8 (15) (2020) 4109–4128.
[73] J. Kreuter, Influence of the surface properties on nanoparticle-mediated transport of drugs to the brain, J. Nanosci. Nanotechnol. 4 (5) (2004) 484–488.
[74] SH Lacerda, JJ Park, C. Meuse, D. Pristinski, ML Becker, A. Karim, et al., Interaction of gold nanoparticles with common human blood proteins, ACS Nano 4 (1) (2010) 365–379.
[75] J. Zhang, T. Yang, W. Huang, Y. Yu, T. Sun, Applications of Gold Nanoparticles in Brain Diseases across the Blood-Brain Barrier, Curr. Med Chem. 29 (39) (2022) 6063–6083.
[76] M. Mahmoudi, Antibody orientation determines corona mistargeting capability, Nat. Nanotechnol. 13 (9) (2018) 775–776.
[77] M. Tonigold, J. Simon, D. Estupinan, M. Kokkinopoulou, J. Reinholz, U. Kintzel, et al., Pre-adsorption of antibodies enables targeting of nanocarriers despite a biomolecular corona, Nat. Nanotechnol. 13 (9) (2018) 862–869.
[78] L. Digiacomo, D. Pozzi, S. Palchetti, A. Zingoni, G. Caracciolo, Impact of the protein corona on nanomaterial immune response and targeting ability, Wiley Inter. Rev. Nanomed. Nanobiotechnol 12 (4) (2020) e1615.
[79] TN Tran, SH Kim, C. Gallo, M. Amaya, J. Kyees, V. Narayanaswami, Biochemical and biophysical characterization of recombinant rat apolipoprotein E: similarities to human apolipoprotein E3, Arch. Biochem Biophys. 529 (1) (2013) 18–25.
[80] GJ Jang, JY Jeong, J. Kang, W. Cho, SY. Han, Size dependence unveiling the adsorption interaction of high-density lipoprotein particles with PEGylated gold nanoparticles in biomolecular corona formation, Langmuir 37 (32) (2021) 9755–9763.
[81] Z. Xia, EE Prescott, A. Urbanek, HE Wareing, MC King, A. Olerinyova, et al., Co-aggregation with Apolipoprotein E modulates the function of Amyloid-beta in Alzheimer's disease, Nat. Commun. 15 (1) (2024) 4695.
[82] C. Soto, EM Sigurdsson, L. Morelli, RA Kumar, EM Castano, B. Frangione, a-sheet breaker peptides inhibit fibrillogenesis in a rat brain model of amyloidosis: implications for Alzheimer's therapy (Bet), Nat. Med 4 (7) (1998) 822–826.
[83] ZA Zhang, X. Xin, C. Liu, YH Liu, HX Duan, LL Qi, et al., Novel brain-targeted nanomicelles for anti-glioma therapy mediated by the ApoE-enriched protein corona in vivo, J. Nanobiotechnology 19 (1) (2021) 453.
[84] R. Dal Magro, B. Albertini, S. Beretta, R. Rigolio, E. Donzelli, A. Chiorazzi, et al., Artificial apolipoprotein corona enables nanoparticle brain targeting, Nanomedicine 14 (2) (2018) 429–438.
[85] CK. Payne, A protein corona primer for physical chemists, J. Chem. Phys. 151 (13) (2019) 130901.
[86] S. Wilhelm, AJ Tavares, Q. Dai, S. Ohta, J. Audet, HF Dvorak, et al., Analysis of nanoparticle delivery to tumours, Nat. Rev. Mater. 1 (5) (2016) 16014.
[87] W. Wei, H. Sun, B. Yang, E. Song, Y. Song, Coronal ApoE Protein Combines with LRP1 to Inactivate GSK3beta that mitigates silica nanoparticle-induced brain lesion, ACS Chem. Neurosci. 15 (4) (2024) 808–815.